Journal of Chromatography A, 1218 (2011) 3153–3158

Contents lists available at ScienceDirect

Journal of Chromatography A

journal homepage: www.elsevier.com/locate/chroma

Factors affecting peak shape in comprehensive two-dimensional gas chromatography with non-focusing modulation

Paul M^cA. Harvey, Robert A. Shellie*

Australian Centre for Research on Separation Science (ACROSS), University of Tasmania, Private Bag 75, Hobart, Tasmania 7001, Australia

ARTICLE INFO

Article history:
Available online 19 August 2010

Keywords:
GC × GC
Pulsed-flow modulation
Peak shape
Peak shape model

ABSTRACT

In the case of a non-focusing modulator for comprehensive two-dimensional gas chromatography (GC × GC), the systematic distortions introduced when the modulator loads the second-dimension column give rise to a characteristic peak shape. Depending on the operating conditions this systematic distortion can be the dominant component of the second-dimension elution profiles in the GC × GC peak. The present investigation involved a systematic investigation of peak shape in pulsed-flow modulation (PFM)–GC × GC. It is shown that low flow ratio can lead to significant peak skewing and increasing the flow ratio reduces the magnitude of peak skewing. Validation of the peak shape model is made by comparison with experimental data. The residuals from the fitting process (normalised to the maximum detector response) vary between –1.5% and +2.6% for an isothermal model and between –1.0% and +3.0% for a temperature-programmed model.

1. Introduction

The ability to modulate the effluent from the first-dimension chromatogram is an important criterion that underpins the successful implementation of any comprehensive two-dimensional gas chromatography (GC × GC) separation. There are three distinct methods available for modulation in GC × GC [1], which include thermal modulation, valve-based modulation, and pneumatic modulation. Valve-based and pneumatic modulation are often considered to be low-cost alternatives for GC × GC because these approaches do not consume liquid cryogen and because the construction of the modulation interface is considerably simpler than a thermal-modulation system. Pneumatic modulation approaches are the most recent additions to the list of GC × GC technologies and these can be categorised as 'differential-flow modulation' [2] or 'simple differential-flow modulation' [3] which has also been called 'pulsed-flow modulation' (PFM) [4,5].

PFM–GC × GC operates by periodically introducing the first-dimension column effluent to the second-dimension column(s) via a series of open-tubular conduits. A PFM–GC × GC modulation interface can built using capillary connection fittings, a gas switching valve and a sufficiently accurate timing device to trigger valve actuation. When the first-dimension column effluent is delivered to the second column by a pressure pulse, the pressure pulse concurrently stops the flow of effluent from the outlet end of the first-dimension column. An inescapable consequence of PFM–GC × GC is that analytes are not focused in the modulator (with respect to the primary column elution volume). To this end, there are two factors that contribute to peak shape in the second-dimension column; first, band dispersion continues within the modulator sample loop during the modulation cycle by diffusion, second the concentration profile of the peak from the first dimension is partially preserved in the resulting second-dimension peak meaning that the elution profile of the first-dimension peak has a significant influence on second-dimension peak shape. Poliak et al. [5] previously alluded to the preserved peak shape in the modulation process, stating that the observed GC × GC peak width is due to a combination of injection width and second-dimension elution time width. The present article further explores this observation and discusses a systematic investigation of peak shape in PFM–GC × GC.

A model of peak shape was developed to illustrate the various contributions that the modulation process imparts upon GC × GC peak shape. Understanding these effects is useful in determining appropriate dimensions of the open-tubular conduits used to set-up a PFM–GC × GC system and aids in carrier gas flow rate choices. Experimental peak data can be de-convoluted using the model into contributions from the first- and second-dimension separations as well as modulation effects.

2. Experimental

All analyses were performed using an Agilent 6890N gas chromatograph (Agilent Technologies, Burwood, Australia). The

* Corresponding author. Tel.: +61 3 6226 7656; fax: +61 3 6226 2858.
E-mail address: Robert.Shellie@utas.edu.au (R.A. Shellie).

0021-9673/$ – see front matter © 2010 Elsevier B.V. All rights reserved.
doi:10.1016/j.chroma.2010.08.029

instrument was fitted with a flame ionisation detector (FID), split/splitless injector and three-channel auxiliary electronic pressure controller. The FID was operated at 340 °C and flow rates were 400 mL/min air, 30 mL/min N_2 and 48 mL/min H_2 (column plus make-up flow). Data were collected at 200 Hz using Agilent MSD Chemstation software. A modulation device was constructed using Valco capillary column unions (tee- and cross-unions) (Grace Davison Discovery Sciences, Rowville, Australia) a three-way switching valve (Parker Hannifin, Castle Hill, Australia) and 0.25 mm i.d. fused silica capillary tubing (Restek, Bellefonte, PA) according to the tubing dimensions reported elsewhere [6]. The first-dimension column was a 15 m × 0.22 mm i.d. column with a 0.25 μm film thickness (BP-1 100% polydimethylsiloxane stationary phase). The second-dimension separation column was a 5 m × 0.25 mm i.d. column with 0.25 μm film thickness (HT-8 8% phenyl (equiv.) polycarborane-siloxane stationary phase). Both columns were from SGE Analytical Science (Ringwood, Australia). The split vent line was 5 m × 0.25 mm i.d. deactivated fused silica capillary tubing. Actuation of the three-way valve was controlled using a purpose built digital timer (SciElex, Kingston, Australia). Agilent MSD Chemstation software was used to signal the digital timer to commence modulation at a precise time.

The temperature program used for the analysis was 40 °C for 2.5 min then 8 °C/min to 252 °C, hold for 5 min. Hydrogen carrier gas was used for all analyses. Standards were obtained from Sigma–Aldrich and solutions prepared in *n*-hexane.

To calculate how the second-dimension column broadening alters the peak shape from the loading profiles, post-modulator peak slices were divided into 1 ms segments. Each of these segments was considered as a separate injection onto the second-dimension column. A time offset was added to each segment corresponding to the delay in elution time of each segment from the first-dimension column as it enters the modulator sample loop. This offset is given by the segment's position within the concentration profile of the peak slice relative to the end of the first-dimension column. Next a suitable Gaussian or modified Gaussian function was used to model a range of band broadening effects on each injection slice segment. Interaction between the different segments of the slice was not considered.

3. Results and discussion

The primary contributions to peak width and shape in PFM–GC × GC separations can be classified as those that can be attributed to chromatographic effects and those that can be attributed to modulation effects. Chromatographic effects are not deeply described here because this information can be found elsewhere [7,8], however modulation effects are discussed in detail. Unlike thermal modulation GC × GC where solutes are focused into narrow bands between the first- and second-dimension columns, Fig. 1 illustrates how the concentration profile from the first-dimension peak is preserved in PFM–GC × GC. Here the reconstructed first-dimension peak profile for a solute having a first-dimension retention time of 13.44 min and peak width (4σ) of 11.4 s. Injection into the second-dimension column occurs every 3 s as indicated by the vertical bars giving a modulation ratio (M_r) of 3.8. Seven individual peak slices are labelled A–G in Fig. 1. One of the more abundant peak slices (slice C) is discussed further. This peak slice is a suitable candidate to illustrate modulation effects. The peak slice has a large change in response during the loading portion of the modulation period and the response is always substantially greater than zero. PFM–GC × GC modulators are non-focusing and although modulation leads to peak compression in time, the shape of this peak slice is maintained as it is delivered to the second dimension. The second-dimension column injection

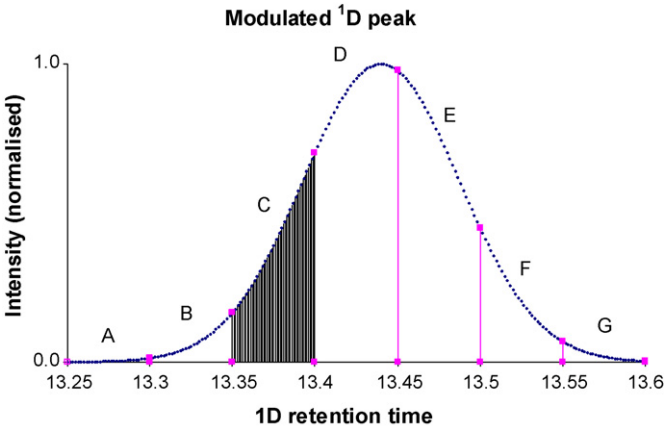

Fig. 1. Reconstructed first-dimension peak profile for a solute having a first-dimension retention time of 13.44 min and peak width (4σ) of 11.4 s. Injection into the second-dimension column occurs every 3 s as indicated by the vertical bars giving a modulation ratio (M_r) of 3.8. A–G represent individual peak slices.

bandwidth can be estimated using Eq. (1) [5,9].

$$\frac{PM}{Flow\ \ Ratio} \quad (1)$$

where *PM* is the modulation period and *Flow Ratio* is the ratio of flush:fill volumetric flow rates in the modulator.

Fig. 2A illustrates the peak compression (in time) for a single peak slice (slice C from Fig. 1) produced from a 3 s modulation period and flow ratio of 100:1 and shows the effect that increasing peak width as a result of second-dimension chromatographic effects (σ_C) has upon peak shape following separation in the second column. In this case the initial width of the compressed peak slice will be 30 ms. In the absence of chromatographic band broadening, this compressed version of the portion of the first-dimension effluent would be exactly maintained and would be reflected by the detector response. However in any real scenario this peak shape is altered by band broadening. The result of the band broadening imparted on each of the segments within the compressed peak slice is also shown in Fig. 2. For a 30 ms wide injection plug of uniform concentration a simplified standard deviation estimate for the sample plug, σ_L, is 8.7 ms. This 8.7 ms estimate ($= 30/2\sqrt{3}$) is obtained from the standard deviation of a uniform (or boxcar) distribution lasting 30 ms and assumes a loading profile of constant concentration. Combining σ_L with the additional broadening during the separation on the second-dimension column (σ_C) gives an estimate of peak width for any peak slice following the second-dimension separation (σ_T). When σ_C is 4 ms (Fig. 2B) the resultant peak has significant asymmetry ($A_s = 0.46$) and retains much of its profile from

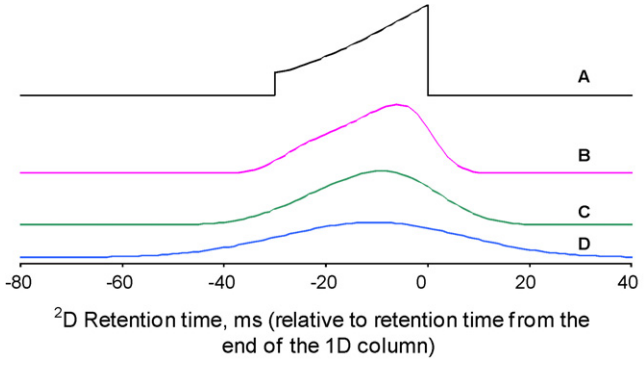

Fig. 2. Single compressed (in time) peak slice produced from a 3 s modulation period and flow ratio of 100:1 and shows the effect that increasing σ (B–C–D) has upon peak shape following separation in the second column.

the first-dimension peak shape. The resulting final peak width, σ_T, is $\sqrt{(4^2 + 8.7^2)} = 9.6$ ms. The width and shape of the peak are consistent with the loading effect being the major contributor towards these parameters. As σ_C is increased to 8 ms (Fig. 2C) the profile has less resemblance to the injection plug. When σ_C is further increased to 16 ms (Fig. 2D) the resulting profile is close to a Gaussian peak ($A_s = 0.95$) with a standard deviation of $\sqrt{(16^2 + 8.7^2)} = 18.2$ ms and second-dimension column broadening is the major component to σ_T. A critical observation associated with the partial retention of the first-dimension peak shape is its effect on second-dimension retention time. Note that the peak apex in each of the cases in Fig. 2 is different. An additional effect on two-dimensional peak shapes is caused by the fact that loading profiles of contiguous first-dimension peak slices are different from one another (Fig. 1A–G). This has a significant influence on the cross-peak shape when the chromatogram is plotted as a two-dimensional colour plot (Fig. 3). In this case the simulated GC × GC peak has a flow ratio of 30. Modulation ratio (M_r) also has a very important influence on peak skewing. Very low M_r will lead to substantial skewing and high M_r reduces it, however there are practical considerations which rule out the use of very high M_r. In this discussion all calculations have been made using a favourable $M_r > 3$. A clear downward trend in the retention times of the peak maxima is expected in the two-dimensional colour plot due to the modulation effects described above. A systematic comparison of varying the flow ratio and second dimension σ_C (Fig. 4) shows that low flow ratio exacerbates this effect and increasing the flow ratio reduces the magnitude of peak-slice to peak-slice retention time differences. The efficiency of the second-dimension column can disguise this peak shape effect. As σ_C increases, the peak skewing becomes less obvious and the contribution of σ_L towards the total peak bandwidth is reduced. As σ_C increases the loading profile has reduced effect on the resulting peak. Examination of the literature reveals that the majority of separations achieved using PFM–GC × GC devices have been performed with a 20–30:1 flow ratio. Coincident with moderate second-column efficiency this moderate flow ratio is in the regime of partial retention of first-dimension peak shape and the contribution to peak shape from modulation effects should not be ignored. Either manual interpretation or automated software-based interpretation of PFM–GC × GC chromatograms needs to be mindful of this peak shape phenomenon, particularly when relatively low flow ratio is combined with low σ_C (noting that σ_L will often be the major component of peak width since $\sigma_C = (t_M(k+1))/\sqrt{N}$ and both k and t_M are small in GC × GC second-dimension separations). Given that the peak shift is predictable suitable software can be expected to adequately compensate for the modulation effect. The peak-picking algorithm needs to be informed to minimise the likelihood of either incorrectly summing the area of closely eluted

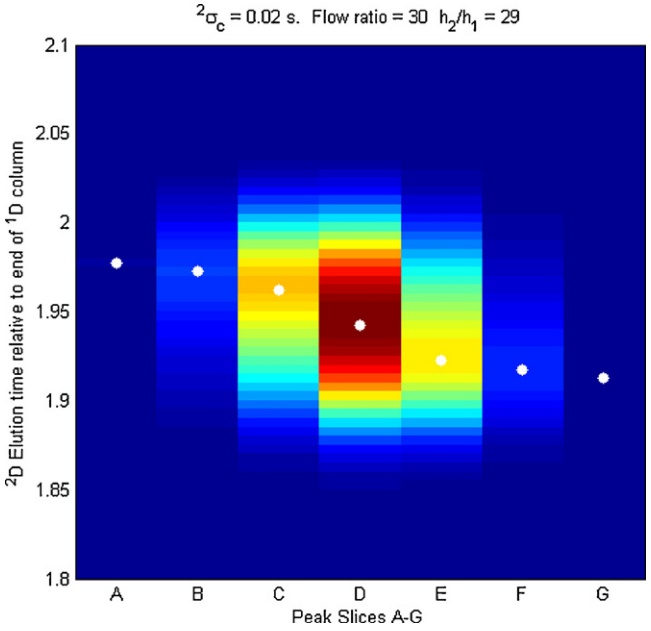

Fig. 3. Two-dimensional projection of all simulated peak slices across a modulated peak. First-dimension profile and modulation period the same as Fig. 1. Flow ratio in modulator = 30. The maximum of each peak slice is marked with a white dot.

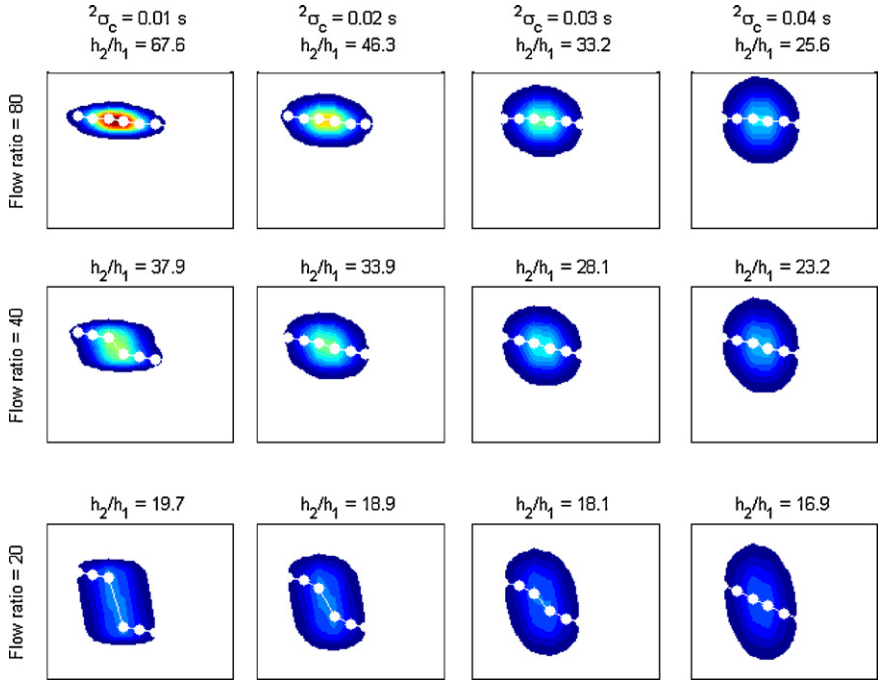

Fig. 4. Systematic comparison of varying the flow ratio highlighting the peak skewing effect and peak amplitude enhancement (h_2/h_1) brought about by modulation. First-dimension peak width (4σ) is 11.4 s, modulation time is 3.0 s, first-dimension retention time in phase with modulation timing.

peaks in the two-dimensional separation space, or incorrectly assigning portions of a single component to two separate peaks. Temperature-programming effects can also cause predictable peak shift [10] that should also be considered for peaks eluting during an oven temperature ramp. It is advisable to employ a flow ratio >30:1 in method development to minimise the modulation (peak shape) effect.

It would be advantageous to be able to predict the amplitude enhancement available in PFM–GC × GC by marrying Eq. (1) with the model shown by Lee et al. [11] to predict peak amplitude enhancement as a function of relative peak widths in the first and second dimensions, respectively. However there are first a few important considerations. Fig. 2D shows the second-dimension peak height/width relationship is influenced only marginally by the modulation effect. Under these circumstances (where σ_C is large compared to σ_L) the observations made by Lee et al. are applicable without change and since performance (N) of the second-dimension column can be reliably predicted it should not be arduous to predict peak amplitude enhancement. However, although it is possible to achieve close to theoretical minimum peak width if an uncoated transfer line is used after the modulator (Poliak et al. [5] have shown 20 ms (FWHH) peaks using a 70 cm × 0.25 mm i.d. transfer line to the detector in a system that had a calculated width of 16 ms), Harvey et al. [6] recently indicated that the concurrent reversal of flow at the first-dimension column outlet following valve actuation may effectively increase the first-dimension flow entering the modulator. Consequently the actual flow ratio is always slightly lower that the theoretical flow ratio. When $\sigma_C < 2\sigma_L$ retention of the original peak profile is likely to be observed and the simple approach of using the relative peak widths in the first- and second-dimension to predict peak amplitude enhancement will not be sufficient. However peak amplitude enhancement can be predicted in all scenarios using the model described here. Fig. 4 highlights the contributions of flow ratio and modulation period (two factors that influence σ_L) towards peak amplitude enhancement (h_2/h_1) in PFM–GC × GC (where h_1 and h_2 are non-modulated and modulated peak heights, respectively). Validation by comparison of experimental data is discussed further below.

Since PFM–GC × GC relies on stopping the flow from the first-dimension column temporarily and periodically, retention times are different in modulated vs. non-modulated experiments so the proposed peak shape models were validated using the following hypothesis:

Since the approach described above can predict peak shapes across all modulations for any given set of system parameters, it is it also possible to determine first and second dimension peak width and time parameters from a GC × GC chromatogram by deconvolving the various contributing factors described above.

The peak shown in the left panel of Fig. 5 was obtained by the analysis of *n*-eicosane that was eluted in an isothermal plateau (252 °C) of a GC × GC temperature-programmed analysis. Six peak descriptors describe a three-dimensional peak in a PFM–GC × GC chromatogram: (i) first-dimension peak width, (ii) second-dimension peak width, (iii) first-dimension retention time, (iv) second-dimension retention times, (v) σ_L (which is determined from the flow ratio, modulation period and first-dimension peak shape), (vi) peak area. Peak shape can be described by a Gaussian function or contain additional terms for other chromatographic shapes such as skew Gaussian, exponentially modified Gaussian (EMG), etc. [12]. For a set of real multidimensional chromatographic data it is possible to accurately project the first-dimension peak profile. Here successive iterations of a simulated three-dimensional peak are compared to the real data until the difference between the real peak and simulated peak is minimised (a multivariate, non-linear minimisation problem). The simulated

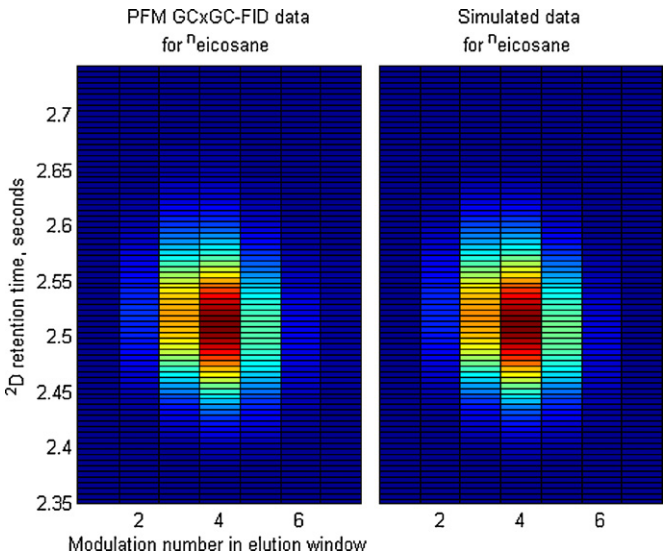

Fig. 5. Left: PFM–GC × GC data for *n*-$C_{20}H_{42}$ eluting on an isothermal (252 °C) plateau in a temperature-programmed method. Right: simulated data.

GC × GC chromatogram was generated using the peak modelling approach described herein from an initial estimate for the six peak descriptors. The projected multidimensional chromatogram was compared directly with the raw GC × GC chromatogram and the peak descriptors were changed until the projected GC × GC chromatogram and the experimental data were in agreement. The specific parameter minimised was the sum of the square of the difference between real and simulated value (i.e. a least squares approach). The projected GC × GC chromatogram for *n*-eicosane after this peak-fitting approach is shown in the right panel of Fig. 5. The two peaks match with outstanding congruity. The residuals from the fitting process vary between –1.5% and +2.6% (normalised to the maximum detector response).

This ability to de-convolute the contributions of modulation and separation efficiency offers both a validation of the new approach for predicting the two-dimensional peak shape as well as a new model for determining first-dimension retention time and width. Previously there have been a number of approaches for determining the first-dimension retention time and width. A simplistic approach uses the most intense second-dimension peak pulse as an estimate of the first-dimension retention time. Shellie et al. [13] briefly described an approach for determining first-dimension retention time, based on fitting the cumulative peak area to a normal cumulative distribution curve. Adcock et al. [14] recently extended this approach and provided a detailed description. Here the new approach for determining first-dimension retention time and peak width was compared with the peak-area method proposed by Adcock et al. The *n*-eicosane peak shown in Fig. 5 is again used for illustrative purposes. Adcock's method was used to determine the first-dimension peak parameters based on summation of all eight modulations during the isothermal plateau. The simplified approach of Adcock et al. using the three most intense modulations was not used in order to permit a fair comparison between methods. Comparison of the two approaches is summarised in Table 1. The best fit using the new model was achieved using a skew Gaussian so Adcock's approach was slightly modified to a skew-Gaussian approximation. The correspondence between the approaches is highly satisfactory and offers additional support to the effectiveness of the approach used here to understand PFM–GC × GC modulation effects.

Table 1
Comparison of predicted peak parameter for *n*-eicosane using different methods.

Approach	First-dimension retention time (min)	σ (first dimension; s)
n-Eicosane (isothermal)		
Adcock et al.	31.116	2.720
Modified Adcock et al. (skew Gaussian)	31.116	2.614 (left)2.808 (right)
Isothermal model (skew Gaussian)	31.112	2.533 (left)2.873 (right)

All observations above are drawn from isothermal/isobaric models. However GC × GC uses a programmed temperature gradient to maximise differences in separation mechanisms in the two separation dimensions [15]. Notwithstanding, it is generally accepted that second-dimension separations are treated as pseudo-isothermal, since the change in temperature during a single modulation period (P_M) is small (often <0.5 °C). Considering a case in which a desirable modulation ratio of four is achieved (where $M_R = 4\sigma/P_M$), the oven temperature is not likely to increase more than a couple of degrees during the elution of the peak from the first-dimension column. However, if temperature effects are ignored the residuals from the fitting process vary between –8% and +17% (normalised to the maximum detector response) for *n*-hexadecane eluting during an 8 °C/min oven temperature ramp. This is considerably worse than the isothermal example above but is still quite satisfactory—in spite of the temperature effect. The reasonable fit for *n*-hexadecane is ascribed to the estimated σ_L peak descriptor (and resulting peak distortion from this parameter) offering compensation for the temperature effect. Although the numerical value for σ_L will now have no physical meaning the ability to estimate the first-dimension retention time and peak width is only slightly compromised.

In the temperature-programmed situation a number of additional steps may be incorporated improve the methodology (and thus determination of the first-dimension peak descriptors) for temperature-programmed operation. For instance the effect of temperature on retention factor is well described by the van't Hoff equation or one of its many variants (Eq. (2)).

$$\ln(K_C) = m \times \frac{1}{T} + c \tag{2}$$

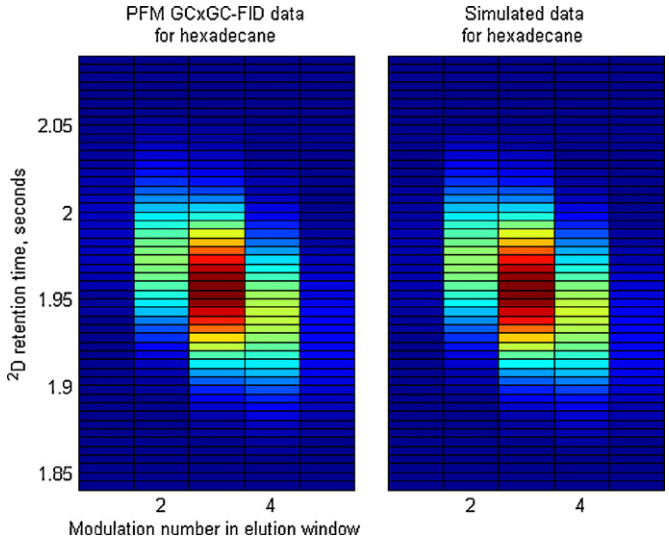

Fig. 6. Left: PFM–GC × GC data and for *n*-hexadecane acquired during an 8 °C temperature-programmed oven ramp. Right: simulated data.

The temperature dependent retention data were obtained from an isovolatility curve [16] for the analyte at a wide range of temperatures. The multivariate, non-linear minimisation now changes marginally from the isothermal case in that a single second-dimension time difference (applied equally across all the modulations) according to the van't Hoff relationship is included. In this manner the temperature dependent second-dimension retention time change is rigorously incorporated. In doing so σ_L once also again has a physical meaning. The peak shown in the left panel in Fig. 6 obtained by analysis of *n*-hexadecane that was eluted in a temperature-programmed GC × GC analysis and is compared in the right hand side with the predicted (projected) response. The residuals from the fitting process vary between –1.0% and +3.0% (normalised to the maximum detector response). By doing so the fit is substantially improved over the isothermal method.

4. Conclusions

With increasing interest in GC × GC instrumentation that is less expensive, bulky, and/or fragile than conventional thermal-modulation systems, the application of PFM–GC × GC has a growing number of supporters. With increasing use of this technology comes an expectation of more systematic investigations of system performance and more studies that improve understanding of the fundamental parameters leading to the chromatogram appearance. Here a systematic investigation of modulation-induced peak shape effects has conclusively shown that significant peak skewing can be expected when a low flow ratio is utilised. Typically, high flow rates are used in the second-dimension column in this type of GC × GC experiment. These are substantially above optimum and lead to reduced efficiency (N), however σ_L is often be the major component of peak width since $\sigma_c = (t_M(k+1))/\sqrt{N}$ and both k and t_M are small in GC × GC second-dimension separations. Therefore minimising the injection pulse width in the second dimension is recommended. Although the peak skewing is somewhat disguised by using a second-dimension column with low efficiency, investigations into improved second-dimension column efficiency are already being made [17]. In the simplest experimental set-up, flow ratio is determined by the flow rates in the first- and second-columns, respectively. High flow ratio can be achieved using low first-dimension column flow rate, or high second-dimension column flow rate. In the simple set-up high flow ratio may have several drawbacks, including high pressures in both primary and secondary columns, either very low flow rates in primary column or very high flow rates in secondary column. Using a dual secondary column arrangement can largely alleviate these drawbacks. The flow parameters described here provide a new guideline for appropriate choice of experimental conditions. The modelling approach is validated by excellent agreement with experimental data and has been shown for both isothermal and temperature-programmed analysis.

Acknowledgements

This work was supported under the Australian Research Council's Discovery funding scheme (project number DP0771893) and Australian Antarctic Science Grant 2930. The generous support of Restek Corporation is gratefully acknowledged.

References

[1] G. Semard, M. Adahchour, J.-F. Focant, Comp. Anal. Chem. 55 (2009) 15.
[2] J.V. Seeley, F. Kramp, C.J. Hicks, Anal. Chem. 72 (2000) 4346.
[3] J.V. Seeley, N.J. Micyus, J.D. McCurry, S.K. Seeley, Am. Lab. 38 (2006) 24.
[4] M. Poliak, M. Kochman, A. Amirav, J. Chromatogr. A 1186 (2008) 189.
[5] M. Poliak, A.B. Fialkov, A. Amirav, J. Chromatogr. A 1210 (2008) 108.
[6] P.M^{c}A. Harvey, R.A. Shellie, P.R. Haddad, J. Chromatogr. Sci. 48 (2010) 245.

[7] C.F. Poole, The Essence of Chromatography, Elsevier Science B.V., Amsterdam, The Netherlands, 2003.
[8] R. Ong, R. Shellie, P. Marriott, J. Sep. Sci. 24 (2001) 367.
[9] P.A. Bueno, J.V. Seeley, J. Chromatogr. A 1027 (2004) 3.
[10] T. Skov, J.C. Hoggard, R. Bro, R.E. Synovec, J. Chromatogr. A 1216 (2009) 4020.
[11] A.L. Lee, K.D. Bartle, A.C. Lewis, Anal. Chem. 73 (2001) 1330.
[12] V.B. Di Marco, G.G. Bombi, J. Chromatogr. A 931 (2001) 1.
[13] R. Shellie, P. Marriott, P. Morrison, L. Mondello, J. Sep. Sci. 27 (2004) 504.
[14] J.L. Adcock, M. Adams, B.S. Mitrevski, P.J. Marriott, Anal. Chem. 81 (2009) 6797.
[15] J.B. Phillips, J. Beens, J. Chromatogr. A 856 (1999) 331.
[16] J. Beens, R. Tijssen, J. Blomberg, J. Chromatogr. A 822 (1998) 233.
[17] P.Q. Tranchida, G. Purcaro, P. Dugo, G. Dugo, P. Dawes, L. Mondello, 7th GC × GC Symposium, Riva del Garda, Italy, 31 May–4 June, 2010.